J|A|C|S
COMMUNICATIONS

Published on Web 12/29/2006

# A Pentanuclear Manganese Single-Molecule Magnet with a Large Anisotropy

Chen-I Yang,[†] Wolfgang Wernsdorfer,[‡] Gene-Hsiang Lee,[§] and Hui-Lien Tsai*,[†]

*Department of Chemistry, National Cheng Kung University, Tainan 701, Taiwan, Republic of China, Laboratoire Louis Néel, CNRS, BP-166, 25 Avenue des Martyrs, 38042 Grenoble, Cedex 9, France, and Instrumentation Center, College of Science, National Taiwan University, Taipei, 106, Taiwan, Republic of China*

Received September 13, 2006; E-mail: hltsai@mail.ncku.edu.tw

Single-molecule magnets (SMMs) have attracted considerable interest because they represent nanoscale magnetic particles with a well-defined size and potential applications in data storage and quantum computation.[1,2] The major goal is to synthesis new SMMs containing a large effective anisotropy energy barrier $U_{eff} \approx |D|S^2$, which results from the combination of a large-spin ground state ($S$) and an Ising-type magnetic anisotropy (negative zero-field splitting parameter $D$).[3] The prototype SMM $[Mn_{12}O_{12}(O_2CCH_3)_{16}(H_2O)_4]$ (**1**) has been extensively studied.[4] It possesses a large energy barrier due to its high spin ground state $S = 10$ and large negative zero-field splitting of $\geq -0.5$ cm$^{-1}$. Few high nuclearity manganese SMMs with spin ground states between $S = 6$ and 83/2 have been reported; however, the values of $U_{eff}$ are relatively small.[5] Thus, many current research objectives for manganese(III) SMMs have been to develop new synthetic approaches and to achieve the associated large single-ion anisotropy.[6] The end-on bridging azide ligand often mediates ferromagnetic exchange between paramagnetic centers,[7] and this property has recently been exploited in the preparation of few SMMs.[5a,c,8]

We herein report a new SMM $(NEt_4)_3[Mn_5O(salox)_3(N_3)_6Cl_2]$ (**2**), which contains a trigonal bipyramid $Mn^{II}_2Mn^{III}_3$ structure with a large magnetic anisotropy approaching a $U_{eff}$ of complex **1**, even so complex **2** is much smaller than **1**. Complex **2** showed AC susceptibility out-of-phase ($\chi_M''$) peaks in the 2−6 K range and large hysteresis loops below 3.0 K. Although a cyanide bridged trigonal bipyramid $\{[Mn^{II}(tmphen)_2]_3[Mn^{III}(CN)_6]_2\}$ (**3**) complex has been reported, the anisotropy energy barrier of complex **3** is small.[9]

Reaction of $MnCl_2 \cdot 4H_2O$, sodium azide, and salicyladoxime ($H_2$-salox) with $NEt_4OH$ in MeOH at room temperature resulted in a deep green solution from which $(NEt_4)_3[Mn_5O(salox)_3(N_3)_6Cl_2]$ formed in 14% yield. The compound crystallizes in rhombohedral space group $R3c$. Crystal structure of the anion of complex **2**[10] is shown in Figure 1. The molecular geometry of $Mn_5$ in **2** is a trigonal bipyramid in which four-coordinate $Mn^{II}$ ions occupy the apical positions and six-coordinate $Mn^{III}$ ions reside in the equatorial triangular plane with a capping $\mu_3$-$O^{2-}$ ion. The $C_3$ axis is perpendicular to the $Mn^{III}_3$ plane and passes through $Mn^{II}$ ions and the central oxygen. Each $Mn^{II}$ ion is linked by three end-on azide bridges to $Mn^{III}$ centers, and a terminal $Cl^-$ completes tetrahedral ligation, while the octahedral ligation of each $Mn^{III}$ ions is completed by a bridging $\eta^1{:}\eta^1{:}\eta^1{:}\mu$-salox$^{2-}$ group, whose phenol ring is bound terminally to a Mn. Bond valence sum (BVS) calculations[11] and the presence of $Mn^{III}$ Jahn−Teller (JT) elongation axes establish the oxidation states of manganese and the protonation level of $O^{2-}$ and salox$^{2-}$ O atoms. In addition, the JT axes (N2−Mn1−N5) of $Mn^{III}$ ions are almost parallel to each other as well as to the crystallographic $C_3$ axis. The shortest intermolecular Mn···Mn distance is 8.65 Å.

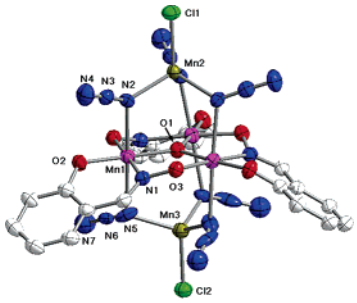


***Figure 1.*** ORTEP representation anion **2** at 30% probability level. Hydrogen atoms have been omitted for clarity.

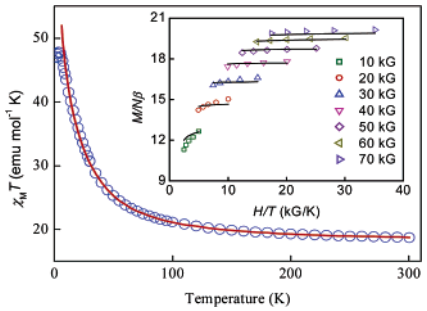


***Figure 2.*** $\chi_M T$ versus $T$ plot for **2** at 100 G. The solid line represents a least-squares fit of the data. Inset: Plot of reduced magnetization versus $H/T$ between 2 and 4 K. Solid lines represent least-squares fit of the data.

The variable temperature DC magnetic susceptibility data were collected for a powder sample of compound **2** in the temperature range of 2−300 K at a magnetic field of 100 G (Figure 2). The value of $\chi_M T$ increase steadily from 18.83 cm$^3$ mol$^{-1}$ K at 300 K as the temperature is lowered, to reach a maximum of 47.82 cm$^3$ mol$^{-1}$ K at 6.0 K, and then decrease to 46.91 cm$^3$ mol$^{-1}$ K at 2.0 K. The $\chi_M T$ value at 300 K is significantly larger than 17.75 cm$^3$ mol$^{-1}$ K, the value expected for a $Mn^{II}_2Mn^{III}_3$ complex with noninteracting metal centers with $g = 2.0$. This behavior clearly indicates the ferromagnetic coupling within **2**, and the small decreasing in $\chi_M T$ at low temperature is likely the result of Zeeman effect, intermolecular interactions, or zero-field splitting in the ground state. In order to describe the coupling within the cluster, the magnetic susceptibility data were fit to the appropriate $\chi_M$ versus $T$ using a $Mn^{II}_2Mn^{III}_3$ Heisenberg−vanVleck model (see Figure 4S in Supporting Information). The data below 6.0 K were omitted in the fitting because zero-field splitting and Zeeman effects likely dominate in this temperature range. The fitting result of DC data in 100 G gave the best fit parameters of $g = 1.98$, $J_1(Mn^{III}-Mn^{II}) = 0.23$ cm$^{-1}$, $J_2(Mn^{III}-Mn^{III}) = 2.41$ cm$^{-1}$. This set of parameters led to a ground state $S_T = 11$ and a first excited state $S = 10$ being closely by at 3.2 cm$^{-1}$.

[†] National Cheng Kung University.
[‡] Laboratoire Louis Néel, CNRS.
[§] National Taiwan University.


10.1021/ja066533a CCC: $37.00 

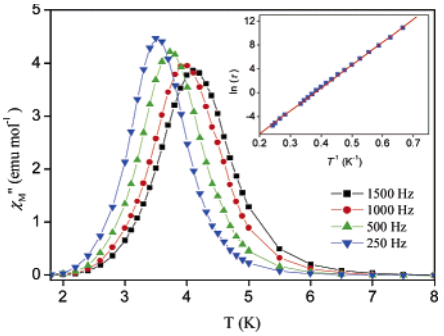


***Figure 3.*** Plots of out-of-phase ($\chi_M''$) AC susceptibility versus $T$ in 3.5 G AC field oscillating at indicated frequencies for **2**. Inset: Arrhenius law fit of the combined AC and DC data.

To identify the ground state, magnetization ($M$) data were collected in the 2.0−4.0 K and 10−70 kG ranges (inset of Figure 2). The results were fitted by using the program ANISOFIT[12] that assumes only the ground state is populated, includes axial zero-field splitting ($D$) and Zeeman interactions, and incorporates a full powder average. The best and equally good fits to the data are obtained with $S = 11$, $g = 1.90$, and $D = -0.22$ cm$^{-1}$ (−0.32 K), $E = -0.071$, and thus, the calculated energy barrier to relaxation ($|D|S_z^2$) is 26.6 cm$^{-1}$ (38.3 K). Attempts to fit the data by using $S = 10$ resulted in unreasonable value of $g = 2.12$.

To investigate whether **2** might be a SMM, AC susceptibility measurements were performed in a 3.5 G AC field oscillating at 250−1500 Hz and with a zero-applied DC field. The frequency dependent amplitude of the in-phase ($\chi_M'T$) signal increased as the temperature was lowered, reached a maximum value at 4.0−5.0 K, and finally approached zero (Figure 5S). The out-of-phase ($\chi_M''$) signals showed clear frequency and temperature dependences (Figure 3). As the frequency of the AC field was changed from 1500 to 250 Hz, the $\chi_M''$ peak shifted from 4.1 to 3.5 K. This frequency dependence of the AC signals suggests that complex **2** is a SMM. Additional relaxation versus time measurements were obtained at a temperature below 3.2 K by the DC magnetization decay versus time measurements (Figure 10S). This gave a set of relaxation times which were combined with the AC data and used to construct an Arrhenius plot. Good fits of the combined AC and DC data allowed us to obtain $\tau_0 = 2.6 \times 10^{-7}$ s and $U_{eff} = 40.3$ K (inset of Figure 3).

In order to probe the anisotropy and quantum tunneling of magnetization (QTM) of complex **2**, single-crystal hysteresis loops and relaxation measurements were performed by using a micro-SQUID setup.[13] Figure 4 presents magnetization ($M$) versus $H$ measurements. The hysteresis loops were strongly sweep rate and temperature dependent and showed steps indicative of QTM. The hysteresis loops become temperature independent below 0.8 K, establishing tunneling between ground state levels. The anisotropy of the spin ground state is obtained from $\Delta H$ between the zero-field step and the first step at 1.1 T yielding a $|D|/g$ value of 0.51 cm$^{-1}$ (Figure 9S). This extreme large anisotropy $|D|/g = 0.51$ cm$^{-1}$ is coming from the almost parallel arrangement of JT axes of Mn$^{III}$ ions in the equatorial triangular plane. At temperatures above about 1 and 1.5 K, other steps appears at 1.2 and 0.6 T, respectively, which are probably due to tunneling via the first excited state being rather close to the spin ground state. The steps at 0.6 and 1.2 T suggest $|D|/g = 0.28$ cm$^{-1}$ for the first excited spin state. Because the latter is very close to the spin ground state, the maximal barrier of $|D|S^2$ is strongly reduced to $U_{eff} = 40.3$ K.

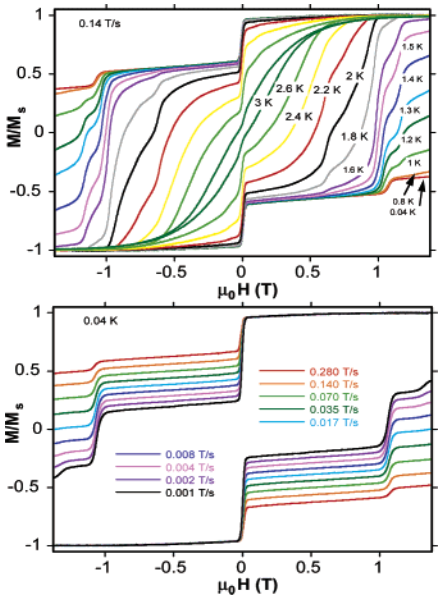


***Figure 4.*** Magnetization hysteresis loops for a single crystal of **2**; (top) from 3.0 to 0.04 K at 0.14 Ts$^{-1}$ scan rate; (bottom) for different scan rates at $T = 0.04$ K.

In conclusion, complex **2** represents a new example of SMMs, with the anisotropy energy $U_{eff}$ of 40.3 K. QTM was observed and allowed us to estimate the anisotropy parameter of the two lowest spin states.

**Acknowledgment.** The magnetic measurements were obtained from SQUID (MPMS XL-7) in NSYSU, and we thank the National Science Council of Taiwan for financial support.

**Supporting Information Available:** Crystallographic details in CIF format, bond valence sums, and magnetism data. This material is available free of charge via the Internet at http://pubs.acs.org.

## References

(1) (a) Leuenberger, M. N.; Loss, D. *Nature* **2001**, *410*, 789−793. (b) Hill, S.; Edwards, R. S.; Aliaga-Alcalde, N.; Christou, G. *Science* **2003**, *302*, 1015−1018.
(2) (a) Sessoli, R.; Tsai, H.-L.; Schake, A. R.; Wang, S.; Vincent, J. B.; Folting, K.; Gatteschi, D.; Christou, G.; Hendrickson, D. N. *J. Am. Chem. Soc.* **1993**, *115*, 1804−1816. (b) Christou, G.; Gatteschi, D.; Hendrickson, D. N.; Sessoli, R. *MRS Bull.* **2000**, *25*, 66−71.
(3) Mirebeau, I.; Hennion, M.; Casalta, H.; Andres, H.; Güdel, H. U.; Irodova, A. V.; Caneschi, A. *Phys. Rev. Lett.* **1999**, *83*, 628−631.
(4) Gatteschi, D.; Sessoli, R. *Angew. Chem., Int. Ed.* **2003**, *42*, 268−297 and references therein.
(5) (a) Murugesu, M.; Habrych, M.; Wernsdorfer, W.; Abboud, K. A.; Christou, G. *J. Am. Chem. Soc.* **2004**, *126*, 4766−4767. (b) Tasiopoulos, A. J.; Vinslava, A.; Wernsdorfer, W.; Abboud, K. A.; Christou, G. *Angew. Chem., Int. Ed.* **2004**, *43*, 2117−2121 and references therein. (c) Ako, A. K.; Hewitt, I. J.; Mereacre, V.; Clérac, R.; Wernsdorfer, W.; Anson, C. E.; Powell, A. K. *Angew. Chem., Int. Ed.* **2006**, *45*, 4926−4929.
(6) Boskovic, C.; Wernsdorfer, W.; Folting, K.; Huffman, J. C.; Hendrickson, D. N.; Christou, G. *Inorg. Chem.* **2002**, *41*, 5107−5118.
(7) Ribas, J.; Escuer, A.; Monfort, M.; Vicente, R.; Cortés, R.; Lezama L.; Rojo, T. *Coord. Chem. Rev.* **1999**, *195*, 1027−1068.
(8) (a) Boudalis, A. K.; Donnadieu, B.; Nastopoulos, V.; Clemente-Juan, M. J.; Mari, A.; Sanakis, Y.; Tuchagues, J.-P.; Perlepes, S. P. *Angew. Chem., Int. Ed.* **2004**, *43*, 2266−2270. (b) Aromí, G.; Parsons, S.; Wernsdorfer, W.; Brechin, E. K.; McInnes, E. J. L. *Chem. Commun.* **2005**, 5038−5040.
(9) Berlinguette, C. P.; Vaughn, D.; Cañada-Vilalta, C.; Galán-Mascarós, J. R.; Dunbar, K. R. *Angew. Chem., Int. Ed.* **2003**, *42*, 1523−1526.
(10) Crystal data for **1**: $C_{45}H_{75}Cl_2Mn_5N_{24}O_7$, $M = 1409.89$, rhombohedral, $R\bar{3}$, $a = 13.4646(2)$ Å, $b = 13.4646(2)$ Å, $c = 59.9213(10)$ Å, $V = 9408.0(3)$ Å$^3$, $T = 150(1)$ K, $Z = 6$; $R(R_w) = 0.0374$ (0.0817).
(11) (a) Brown, I. D.; Altermatt, D. *Acta Crystallogr., Sect. B* **1985**, *41*, 244−247. (b) Liu, W.; Thorp, H. H. *Inorg. Chem.* **1993**, *32*, 4102−4105.
(12) Shores, M. P.; Sokol, J. J.; Long, J. R. *J. Am. Chem. Soc.* **2002**, *124*, 2279−2292.
(13) Wernsdorfer, W. *Adv. Chem. Phys.* **2001**, *118*, 99−190.

JA066533A